Mechanisms responsible for the photocurrent in bacteriorhodopsin

Eleonora Alfinito[*]

Dipartimento di Ingegneria dell'Innovazione, Università del Salento, via Monteroni, I-73100 Lecce, Italy
and CNISM, Via della Vasca Navale, 84-00146 Rome, Italy

Lino Reggiani[†]

Dipartimento di Matematica e Fisica, "Ennio de Giorgi," Università del Salento, via Monteroni, I-73100 Lecce, Italy
and CNISM, Via della Vasca Navale, 84-00146 Rome, Italy

Recently, there has been growing interest in the electrical properties of bacteriorhodopsin (bR), a protein belonging to the transmembrane protein family. Several experiments pointed out the role of green light in enhancing the current flow in nanolayers of bR, thus confirming potential applications of this protein in the field of optoelectronics. By contrast, the mechanisms underlying the charge transfer and the associated photocurrent are still far from being understood at a microscopic level. To take into account the structure-dependent nature of the current, in a previous set of papers we suggested a mechanism of sequential tunneling among neighboring amino acids. As a matter of fact, when irradiated with green light, bR undergoes a conformational change at a molecular level. Thus, the role played by the protein tertiary-structure in modeling the charge transfer cannot be neglected. The aim of this paper is to go beyond previous models, in the framework of a new branch of electronics we call proteotronics, which exploits the ability of using proteins as reliable, well-understood materials for the development of novel bioelectronic devices. In particular, the present approach assumes that the conformational change is not the unique transformation the protein undergoes when irradiated by light. Instead, the light can also promote an increase of the protein state free energy that, in turn, should modify its internal degree of connectivity. This phenomenon is here described by the change of the value of an interaction radius associated with the physical interactions among amino acids. The implemented model enables us to achieve a better agreement between theory and experiments in the region of a low applied bias by preserving the level of agreement at high values of applied bias. Furthermore, results provide new insights on the mechanisms responsible for bR photoresponse.

PACS number(s): 87.15.Pc, 87.14.et, 87.19.R−

I. INTRODUCTION

Bacteriorhodopsin (bR) is the best-known protein in the family of opsins, proteins conjugated with a molecule of retinal and able to convert visible light into electrostatic energy [1]. This protein is found in a primeval organism, the *Halobacterium salinarum*, specifically in a part of its cell membrane called the purple membrane (PM), because of its color. This membrane, 5 nm thick, is a natural thin film, essentially constituted of a few lipids and these proteins organized in an hexagonal lattice [2].

A large number of studies have been carried out on bR in the field of biophysics and physicochemistry [3–5], and many aspects have been unveiled. As relevant examples we cite: (i) the photoinduced isomerization of the retinal embedded in bR [6], (ii) the conformational change of bR associated with the retinal isomerization [7], and (iii) the importance of environmental conditions in the photocycle development [8,9].

Patches of PM have been used for several purposes: to produce metal-protein-metal junctions [10–12], to perform conductive atomic force microscopy (c-AFM) investigations [13,14], to develop solar cells of new generation [15], and so on. As a matter of fact, films of bR resist thermal, electrical, and mechanical stress [10–14] and show a substantial pho-

tocurrent when irradiated by a visible (green) light [10,12,16]. Therefore, bR can be used as an optoelectrical switch to convert radiant energy into electrical energy [15], in pollutant remediation systems [17], to produce optical memories [18], to control neuronal and tissue activity [19,20], and so on.

The commonly accepted view concerning protein activation is the following: A photon is absorbed by the retinal molecule contained in each protein, which then causes the bending of this molecule. As a consequence, the protein undergoes a change of its tertiary structure, following a cycle of transformations that culminates in the release of a proton outside the cell membrane. Finally, reprotonization of the retinal molecule by Asp96 restores the native configuration. Some crystallographic investigations have been performed on this protein to determine its configuration in the different steps of the cycle [8]. This is a particularly hard task, since the x-ray radiation could modify the protein structure, and only recently has the puzzle of many contradictory results begun to be examined [21]. At present, a rather complete description of the protein is given only for the native and the active L state [22,23].

Measurements of the protein current-voltage (I-V) characteristics were reported in several papers [10–14]. To this purpose, samples made of patches of PM were anchored on a conductive substrate and connected to an external circuit. The connection was made with (i) an extended transparent conductive contact [10–12] and (ii) a tip of a c-AFM [13,14]. In both cases, the measured current was found to be quasiohmic at the lowest bias and strongly superlinear at increasing bias.

———————
[*]eleonora.alfinito@unisalento.it; http://cmtg1.unile.it/eleonora1.html

[†]lino.reggiani@unisalento.it

Furthermore, when the sample was irradiated with green light [10,12], a significant photocurrent was observed. There was clear proof that the charge transfer is mainly due to the protein [10,12]. There was also a high resistance channel due to the lipid membrane, which is detected in experiments involving a membrane deformation [13,24]. In the absence of membrane deformation, this channel can be neglected. The charge transfer through the protein was attributed to a tunneling mechanism [10,13,24,25]. In particular, the presence of a current (in dark) well above possible leakage components and of a photocurrent (in light) supports the hypothesis of a mechanism of charge transfer intrinsically dependent on the protein tertiary structure [24–32].

The interaction of electromagnetic fields with biological matter long has been the object of many investigations, mainly for the damages produced by ionizing radiations. As far as we know, sunlight that reaches the Earth is largely composed of nonionizing radiation whose main effect on biological matter is heating. In particular, for proteins, this should lead to a global energy enhancement, regardless of the protein-specific conformational state, as confirmed by recent experiments showing the critical role of temperature in current measurements [12]. Therefore, we conjecture that in a sample of proteins, like a patch of purple membrane, light gives rise to different effects. From one side, the retinal modification with the consequent conformational change from the native to the active state and, from another side, a net transfer of energy to the whole protein with a consequent increase of its free energy. As a general issue, both these effects should contribute to the protein activation.

The present paper addresses this issue by accounting simultaneously for these two effects in a computational-theoretical model called impedance network protein analog (INPA). This approach describes the electrical characteristics of a protein by using a network of impedances. In previous investigations, the local interaction of a photon with the retinal has been investigated by considering the corresponding change of the network structure. The novelty of the present paper consists in the further introduction of a global energy increase of the whole protein due to the incident light. This is described by a change of the network connectivity both of the native and the active states.

The methodological approach we follow points to the integration of different disciplines (molecular biology, physics, electronics) to develop a new generation of electronic devices within a nanobiotechnology. This interdisciplinary approach is leading to an entirely new discipline which we call *proteotronics* [33].

The paper is organized as follows. Section II summarizes the main steps of the INPA model and describes the improvements introduced on the basis of the dynamical evolution of the protein energy landscape. Section III reports and discusses the main results and suggests the opening of new perspectives. Major conclusions are summarized in Sec. IV.

II. THEORETICAL MODEL

The INPA model is based on a percolative approach that describes the protein as a network of links and nodes. A node represents a single amino acid and its spatial position is the same of the corresponding C_α atom. A link joins a couple of nodes and represents the interaction between amino acids [34–36]. The protein structure in its native or active state is taken by public databases or homology modeling [22,37], thus the node configuration reproduces the protein backbone. Then, pairs of nodes are connected with the rule that they must be be closer than an assigned interaction radius, R_c. In this way, the number of links, N, depends on the value of R_c and is in the range $0 \leqslant N_{aa} \leqslant N_{aa}(N_{aa} - 1)/2$, with N_{aa} the number of amino acids pertaining to the given protein. In the present case, the macroscopic quantity of interest is the static I-V characteristic. Therefore, the network is drawn like an electrical circuit where an elementary resistance, $R_{i,j}$, is associated with each link between nodes i and j. Explicitly,

$$R_{i,j} = \frac{l_{i,j}}{\mathcal{A}_{i,j}} \rho, \tag{1}$$

where $\mathcal{A}_{i,j} = \pi(R_c^2 - l_{i,j}/4)$ is the cross-sectional area between two spheres of radius R_c centered on the i-th and j-th nodes, respectively, $l_{i,j}$ is the distance between the sphere centers, and ρ is the resistivity.

By positioning the input and output electrical contacts, respectively, on the first and last nodes (more structured contacts can be envisioned) for a given applied bias (current or voltage operation modes according to convenience), the network is solved within a linear Kirchhoff scheme and its global resistance, R, is calculated [24–33]. Accordingly, this network produces a parameter-dependent static I-V characteristic for the single protein, based on the standard relation:

$$V = RI. \tag{2}$$

To account for the superlinear behavior of current at increasing voltages, a tunneling mechanism of charge transfer is included. In doing so, a stochastic approach within a Monte Carlo scheme [24,25,27,29–32] is used. In particular, following the Simmons model [38], a mechanism containing two possible tunneling processes, a direct tunneling (DT) at low bias and a Fowler-Nordheim tunneling (FN) at high bias, is introduced. Therefore, the resistivity value of each link is chosen between a low value $\rho_{\min}$, taken to fit the current at the highest voltages, and a high value $\rho(V)$, which depends on the voltage drop between network nodes as:

$$\rho(V) = \rho_{\text{MAX}} \quad (eV < \Phi), \tag{3}$$

$$\rho(V) = \rho_{\text{MAX}} \left(\frac{\Phi}{eV} \right) + \rho_{\min} \left(1 - \frac{\Phi}{eV} \right) \quad (eV \geqslant \Phi), \tag{4}$$

where ρ_{MAX} is the maximal resistivity value taken to fit the I-V characteristic at the lowest voltages (ohmic response) and Φ is the height of the tunneling barrier between nodes. The transmission probability of each tunneling process is given by [25,27]:

$$P_{i,j}^{\text{DT}} = \exp\left[-\alpha \sqrt{\left(\Phi - \tfrac{1}{2} eV_{i,j} \right)} \right] \quad (eV_{i,j} < \Phi), \tag{5}$$

$$P_{ij}^{\text{FN}} = \exp\left[-\alpha \frac{\Phi}{eV_{i,j}} \sqrt{\frac{\Phi}{2}} \right] \quad (eV_{i,j} \geqslant \Phi), \tag{6}$$

where $V_{i,j}$ is the potential drop between the couple of i, j amino acids, $\alpha = \frac{2l_{i,j}\sqrt{2m}}{\hbar}$, and m is the electron effective mass, here taken as the same of the bare value. The DT superscript refers to the low-bias, quasiohmic response and the FN subscript refers to the high-bias, superohmic response.

III. RESULTS AND DISCUSSION

By construction, both the current response at very low and very high bias exhibit an ohmic behavior with values of the corresponding resistance differing for several orders of magnitude. This model was successfully used to reproduce the experiments of Ref. [13]. The inputs parameters were $R_c = 6$ Å, $\Phi = 219$ meV, $\rho_{\mathrm{MAX}} = 4 \times 10^{13}$ Ω Å, for the low field resistivity and $\rho_{\mathrm{min}} = 4 \times 10^{4}$ Ω Å for the high field resistivity. The protein tertiary structure was taken from the protein database [22], specifically the 2NTU entry, an x-ray crystallographic measurement for the bR native state.

The agreement between calculations and experiments was found to be satisfactory, also reproducing the current modifications due to the membrane indentation by the c-AFM tip [24]. On this basis, we found reasonable to take the same input to fit the response of the protein in light. At present, the only crystallographic entry describing the complete protein in an active state is 2NTW, which gives account of the L state (henceforth called the active state) of bR. This state is sensitive to the 550-nm light and precedes the M state (410 nm), which corresponds to a proton releasing. In the I-V measurements, the proton releasing was not monitored and the current measured was only attributed to electron transfer [10]. When the activated configuration was used as input to fit the current response in the presence of light, the agreement with experiments was less satisfactory than that in dark. A possible way to overcome this drawback is to assume that the presence of light modifies not only the protein structure but also its connectivity properties. In the INPA model this modification is accounted for by changing the value of the interaction radius. To this purpose, Fig. 1 reports the role of the interaction radius in the calculation of the resistances of the native and active states. Numerical data are obtained at
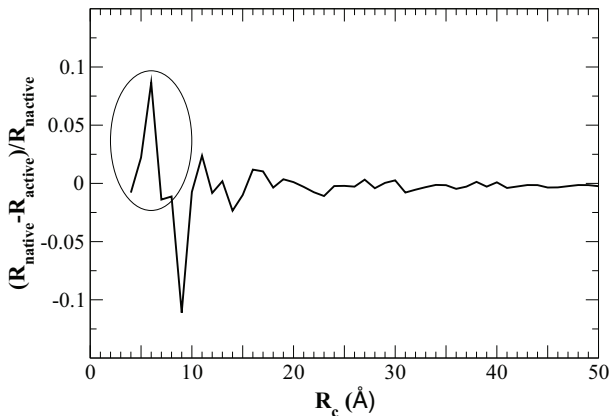

FIG. 1. Relative resistance variations vs the interaction radius, R_c, for bR in the native and active state. The ellipse indicates the region of R_c values whose trend is in agreement with experiments.
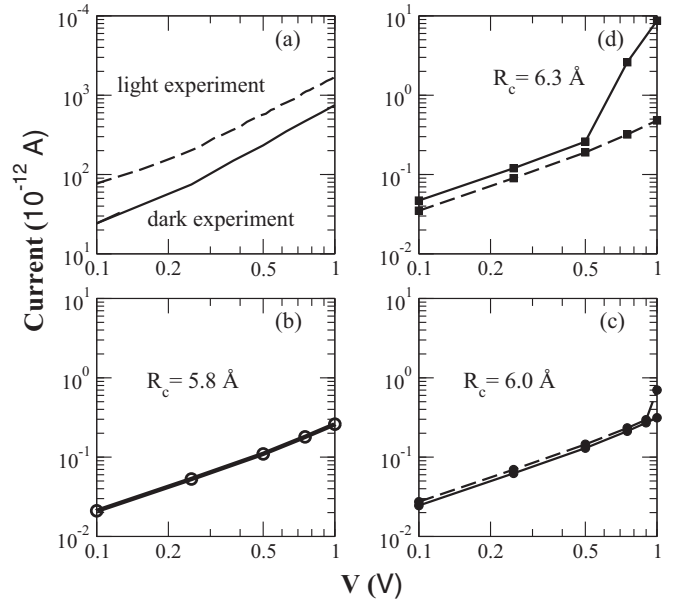

FIG. 2. I-V characteristics of bR. Panel (a) reports the experiments carried out on nanolayers samples [10]. Panels (b)–(d) refer to data calculated within the INPA model (single protein) for the different values of R_c reported in the figures. Symbols refer to numerical calculations; lines are guides to the eyes. Dashed lines and superimposed symbols refer to the active state and continuous lines and superimposed symbols to the native state. For $R_c = 5.8$ Å the I-V characteristics are found to coincide for native and active states.

very low voltages, where the ohmic regime strictly holds, and reflect the protein topology. The main results of Fig. 1 are (i) the general low resolution between these states and (ii) the presence of two regions in which the resolution is best appreciable, around $R_c = 6$ Å and $R_c = 9$ Å. The experiments are in agreement with $R_c = 6$ Å.

In the following the protein current responses are numerically analyzed for several values of R_c around 6 Å. In particular, simulations for the single protein are performed for the three values $R_c = 5.8$, 6.0, and 6.3 Å and for both the native and active states. Results are reported in Fig. 2 with Fig. 2(a) reporting the experimental data carried out in a bR macroscopic sample [10] in dark and light. For a given protein state, Fig. 2 shows a current enhancement by increasing R_c from 5.8 to 6.3 Å. Furthermore, at increasing R_c, the differences between the current response in dark and light are more and more marked.

The above results suggest that the activation mechanism of a *macroscopic sample* of bR can be described within the *single* protein model by using (i) a conformational change (from the 2NTU to the 2NTW structure) and (ii) a connectivity change (i.e., a variation of the network interaction radius).

More specifically, we can envision a twofold mechanism of photon absorption by the retinal and by the whole protein. The former is responsible of the conformational change and the latter of a global energy increase of the protein. Notice that, in accordance with experiments [12], the global energy increase is coherently used by the protein sample in enhancing its photocurrent response. In other words, the electromagnetic
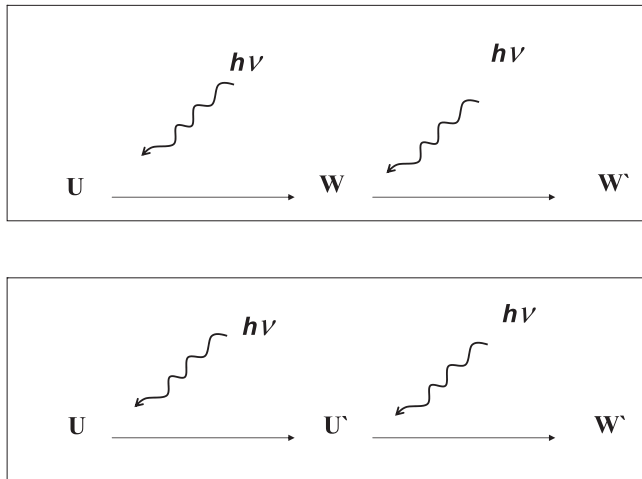
FIG. 3. Schematic representation of the energy evolution by absorption of photons in a bR molecule. Upper panel depicts the conformational change from the native state U to an active state W induced by the absorption of a photon by the retinal and a successive global energy increase from W to W' induced by the absorption (from the whole protein) of other photons. Lower panel depicts an alternative possibility when the absorption of photons induces a global energy increase from U to U' of the native state and a successive absorption process induce a conformational change from U' to the energy level W' of the active state.

radiation impinging on the protein may produce the global effect of an energy gain anyway, while the local interaction of a photon with the retinal triggers the conformational change when the protein is in its native state. These mechanisms associated with photon absorption are schematically depicted in Fig. 3. On the one hand, when the native state, say U, becomes an active state, say W, a further irradiation should enhance the global energy of the active state. In this way, the active state is promoted to an upper energy value W'. On the other hand, when the U state does not undergo a conformational change, its energy level can be promoted to an upper value U'; a further dose of light may drive this state to an active state W'.

Among the different ways used to describe the protein energy landscape at different stages of the folding, one of the most accepted is the rugged funnel diagram [39]. In this diagram, the protein folds from the molten state to the native (stable) state following many possible folding routes toward the minimum of a funnel-like energy surface. When the protein runs down in the energy funnel, it loses the spurious bonds and enforces those stabilizing the minimal-energy configuration [39]. In doing so, it also reaches the minimum of the configurational entropy. Furthermore, the phase transition from a stable state at low energy to a stable state at higher energy is depicted in terms of a tunneling between the minima of a multiwell energy landscape [40]. As energy increases, the spurious connections do again appear and the protein can explore more microstates. In a very schematic way, this mechanism is pictured in Fig. 4 where a couple of funnels representing the native and an active state are superimposed. The conformational change corresponds to the transition from a funnel to another one. The minimal energy between the two
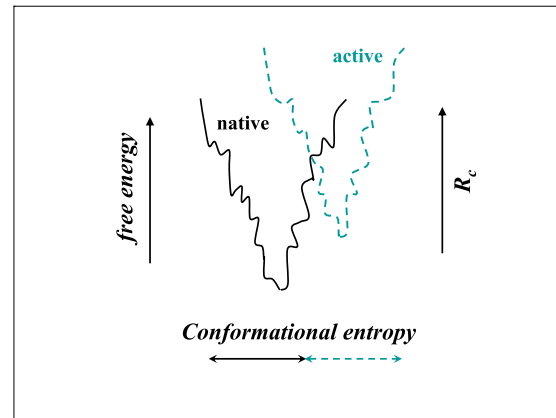

FIG. 4. (Color online) Schematic representation of the free-energy funnel landscape for native and active states. The minima of the free-energy corresponds to a minimum of the conformational entropy that measures the number of available microscopic states. The increase of connectivity at increasing free energy is depicted by the increase of the interaction radius R_c.

funnel stable minima is of the order of the eV. Otherwise, by raising the energy of the protein in the native state, it is possible to reach the overlapping region of the two funnels. Here the transition from the native to the active state can occur without energy supply.

Within the INPA model, the mechanism of energy increase is described by an increase of the R_c value. As a consequence, the network becomes more connected, which implies an increase of the pathways for tunneling and of the number of possible current channels. This, in turn, leads to an increase of the instantaneous current fluctuations, as reported in Fig. 5. Here the current fluctuations observed from simulations are reported for the active state, with an applied bias of 0.75 V and for the two R_c values of 5.8 and 6.3 Å.

Following this scheme, the current response of samples made by monolayers of bR has been fitted by using a binary mixture of native and active states, the percentages of each state being a function of the R_c value [28]. Specifically, a good fit of the experimental data [10] is obtained by using (i) for
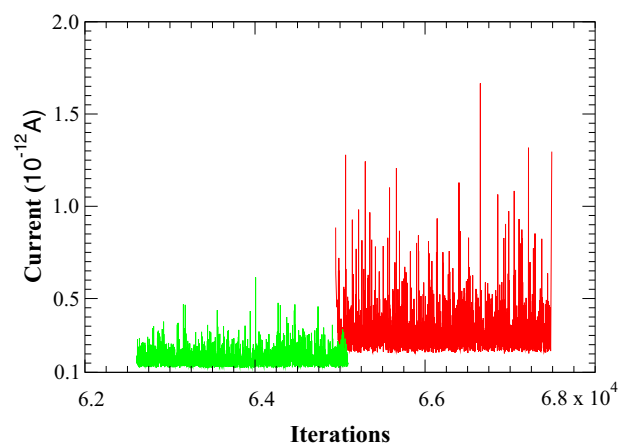

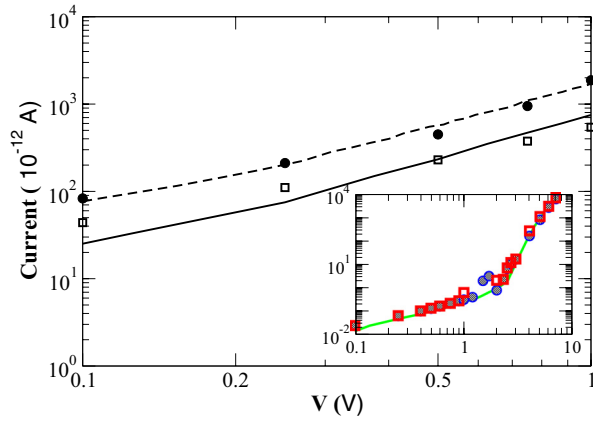FIG. 5. (Color online) Current evolution during the simulation for bR in its active state at different values of R_c.

FIG. 6. (Color online) I-V characteristics calculated by using different mixtures of bR native and active states. Full circles refer to the mixture 4% of native states and 96% of active states with $R_c = 6.3$ Å. Open squares refer to a pure native state with $R_c = 5.8$ Å. Continuous (dashed) line refers to experimental data [10] in dark (light) in the bias range 0.1/1 V. In the inset the continuous line refers to experimental data in dark [13], in the bias range 0.1/10 V. Circles refer to data calculated with the pure native state with $R_c = 6.0$ Å, and squares refer to data calculated with the mixture of 60% of native states and 40% of active states, with $R_c = 6.0$ Å.

the sample in light, $R_c = 6.3$ Å and a binary mixture of 96% of 2NTW and a 4% of 2NTU, and (ii) for the sample in dark, $R_c = 5.8$ Å and 100% of 2NTU.

The c-AFM experiment, performed in the absence of direct light [13], was previously fitted within a very good accuracy on the full bias range by using $R_c = 6.0$ Å and 100% of the 2NTW native state [24]. Since in these experiments one cannot exclude the presence of a certain amount of proteins in the active state, in agreement with a value of R_c larger than the threshold value $R_c = 5.8$ Å , here the fit with experiments is tested by using binary mixtures with an increasing percentage of active states. The fit is found to be sufficiently accurate with a percentage of active state not larger than 40%. Figure 6 reports (i) the experimental data [10,13] and (ii) the single-protein data rescaled by using the formula

$$I_S = A\left(I_n \times n_n + I_a \times n_a\right), \qquad (7)$$

where I_S indicates the sample current, A is a numerical constant of the order of 10^4 used to scale the single protein current to the macroscopic data, $I_{n/a}$ is the current of the single protein calculated with the native-active configuration, $n_{n/a}$ is the fraction of native-active protein expected in the sample. Of course, for a pure state, this formula reduces to the simple proportional rescaling:

$$I_S = A I_{n/a}. \qquad (8)$$

Figure 7 reports the concentration of active 2NTW states in the samples versus the corresponding R_c values to be used in simulations. Symbols refer to values used in simulations and the dashed curve is a fitting obtained from a sigmoidal Hill-like function that is commonly used in biochemistry to describe the percentage of proteins activated by a ligand. Its validity in fitting several different physicochemical reactions
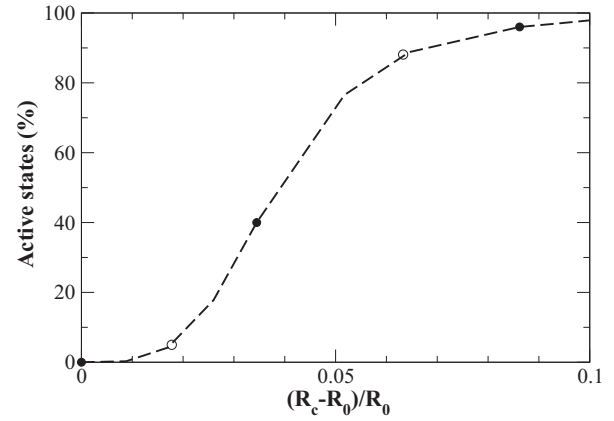

FIG. 7. Percentage concentration of proteins in the active state for the different values of the interaction radius to be considered in simulations. Full circles refer to the values used in Fig. 6, the dashed line is the fitting obtained with Eq. (7), and the empty circles refer to values intermediate between the experiments reported in Ref. [10], see text.

is well known [41] and is written:

$$f(x) = \frac{x^\alpha}{b + x^\alpha} \times 100,$$
$$x = \frac{R_c - R_0}{R_0}, \qquad (9)$$

where f is the percentage of proteins in the active state and $R_0 = 5.8$ Å. For $x^a = b$, half of the proteins in the sample have changed their configuration. Here, the best-fitting parameters are $a = 3.91$ and $b = 2.87 \times 10^{-6}$, i.e., $b^{1/\alpha} = 0.038$. The full circles reproduce the experiments reported in Fig. 7. For the case of the experiments in Ref. [10], further binary mixtures with the percentages suggested by Eq. (9) (open circles) have been tested to be consistent with experiments but to a less quantitative resolution of the photocurrent.

In the present context, the meaning of the function f is the following: for an increasing number of photons impinging onto the sample, the free energy of the protein grows and, as a consequence, the value of R_c also grows. With R_c also the percentage of proteins moved to the active state grows because some of the photons hit the retinal. Finally, for R_c larger than about 7 Å all the proteins in the sample are in the active state. Further, the amount of photons may only improve the free energy of the protein in the active state and the internal degree of connections.

IV. CONCLUSIONS

The paper investigates the mechanisms responsible for the photocurrent exhibited by monolayer samples of bacteriorhodopsin in the presence of an impinging green light. To this purpose, use is made of the INPA model implemented to account for the change of connectivity of the single protein associated with the presence of the light. Previous results provided a satisfactory interpretation of a set of accurate measurements, performed with the c-AFM technique, in nanolayer samples and in the absence of direct light. Accordingly, experiments were interpreted on the basis of

the tertiary structure associated with the native state of the single protein. However, a less satisfactory agreement was obtained in the region of low voltages when the same approach was applied to the case of monolayer samples of bR in the presence of light and thus taking the tertiary structure of the protein in its active state. To overcome this drawback, here we consider also the change in the connectivity of the protein state consequent to the enhancement of the free-energy level of the single protein induced by the presence of the light. The increase in connectivity is accounted for by an increase of the value of the interaction radius, R_c, already introduced to correlate the electrical properties with the tertiary structure of the protein. Accordingly, the new model interprets the photocurrent using a binary mixture of results pertaining to the native and active structures with the proper values of R_c [28]. Specifically, a satisfactory fit of experiments on nanolayers [10] is obtained by using (i) for the sample in light, $R_c = 6.3$ Å and a binary mixture of 96% of 2NTW and of 4% of 2NTU, and (ii) for the sample in dark, $R_c = 5.8$ Å and 100% of 2NTU. The c-AFM experiments, performed in the absence of direct light, are quite finely reproduced by using a binary mixture containing up to 40% of 2NTW and $R_c = 6.0$ Å (see Fig. 6). Therefore, the implemented model enables us to achieve a better agreement between theory and experiments in the region of low applied bias and does not modify previous findings at high values of applied bias.

We notice that the process of protein activation, in particular for opsins, is still a very open topic [39,40] and the present approach aims to provide a further step for a better understanding of the subject. Presenting a quantitative link between the intensity and frequency of incident light to the interaction radius R_c of the INPA model and the relative mixture of native and active states is beyond the scope of the paper. To this purpose, further experiments monitoring the protein response to different light intensity and frequency conditions are necessary to extend and validate the model. Environmental effects, different from the presence of light, like temperature, the value of the pH, etc., should be responsible for other activation mechanisms. Accordingly, more experiments and structural information are necessary, and the present results should give a further motivation to stimulate new experiments and formulate new theories. Finally, this research exploits the trend in which different emerging disciplines can converge in a new branch of science that we recently introduced as proteotronics [33]. Indeed, proteotronics aims to develop new devices based on the sensing properties of proteins. In doing so, protein responses to external stimuli can be better understood and used to devise biodevices of relevant importance in applied sciences.

[1] R. H. Lozier, R. A. Bogomolni, and W. Stoeckenius, Biophys. J. **15**, 955 (1975).
[2] A. Corcelli, M. Colella, G. Mascolo, F. P. Fanizzi, and M. Kates, Biochemistry **39**, 3318 (2000).
[3] G. Varo, L. S. Brown, R. Needleman, and J. K. Lanyi, Biophys. J. **76**, 3219 (1999).
[4] M. Etzkorn *et al.*, Structure **21**, 394 (2013).
[5] M. Yoshino *et al.*, J. Phys. Chem. B **117**, 5422 (2013).
[6] R. Gonzàlez-Luque *et al.*, Proc. Natl. Am. Soc. **97**, 9379 (2000).
[7] S. Subramaniam and R. Henderson, Nature **406**, 653 (2000).
[8] H. Luecke, Biochim. Biophys. Acta **1460**, 133 (2000).
[9] T. Kouyama and A. Nasuda-Kouyama, Biochemistry **28**, 5963 (1989).
[10] Y. Jin, N. Friedman, M. Sheves, T. He, and D. Cahen, Proc. Natl. Am. Soc. **103**, 8601 (2006).
[11] I. Ron *et al.*, J. Am. Chem. Soc. **132**, 4131 (2010).
[12] L. Sepunaru, N. Friedman, I. Pecht, M. Sheves, and D. Cahen, J. Am. Chem. Soc. **134**, 4169 (2012).
[13] I. Casuso, L. Fumagalli, J. Samitier, E. Padros, L. Reggiani, V. Akimov, and G. Gomila, Phys. Rev. E **76**, 041919 (2007).
[14] S. Mukhopadhyay, S. R. Cohen, D. Marchak, N. Friedman, I. Pecht, M. Sheves, and D. Cahen, ACS Nano. **8**, 7714 (2014).
[15] V. Renugopalakrishnan *et al.*, J. Phys. Chem. C. **118**, 16710 (2014).
[16] A. V. Patil, T. Premaruban, O. Berthoumieu, A. Watts, and J. J. Davis, J. Phys. Chem. B **116**, 683 (2012).
[17] G. Dai, L. M. Chao, and T. Iwasa, Adv. Mat. Res. **955**, 415 (2014).
[18] N. Hampp, Chem. Rev. **100**, 1755 (2000).
[19] S. Q. Lima and G. Miesenöck, Cell **121**, 141 (2005).
[20] K. Deisseroth, Nat. Methods **8**, 26 (2010).
[21] C. Wickstrand, R. Dods, A. Royant, and R. Neutze, Biochimica et Biophysica Acta (BBA)-General Subjects **1850**, 536 (2015).
[22] H. M. Berman *et al.*, Nucl. Acids Res. **28**, 235 (2000).
[23] J. K. Lanyi and B. Schobert, J Mol Biol. **365**, 1379 (2007).
[24] E. Alfinito, J.-F. Millithaler, and L. Reggiani, Phys. Rev. E **83**, 042902 (2011).
[25] E. Alfinito and L. Reggiani, Europhys. Lett. **85**, 68002 (2009).
[26] E. Alfinito, C. Pennetta, and L. Reggiani, AIP Conf. Proc. **1137**, 115 (2009).
[27] E. Alfinito and L. Reggiani, J. Phys: Conf. Ser. **193**, 012107 (2009).
[28] E. Alfinito, J. F. Millithaler, L. Reggiani, N. Zine, and N. Jaffrezic-Renault, RSC Adv. **1**, 123 (2011).
[29] E. Alfinito, J. Pousset, L. Reggiani, and K. Lee, Nanotechnology **24**, 395501 (2013).
[30] E. Alfinito and L. Reggiani, J. Phys: Condens. Matter **25**, 375103 (2013).
[31] E. Alfinito and L. Reggiani, J. Appl. Phys. **116**, 064901 (2014).
[32] E. Alfinito, J. Pousset, and L. Reggiani, J. Phys. Conf. Ser. **490**, 012134 (2014).
[33] E. Alfinito, L. Reggiani, and J. Pousset, *Sensors*, Lecture Notes in Electrical Engineering Vol. 319, edited by D. Compagnone *et al.* (Springer International Publishing, 2015), pp 3–7.
[34] E. Alfinito, V. Akimov, C. Pennetta, L. Reggiani, and G. Gomila, AIP Conf. Proc. **800**, 381 (2005).

[35] V. Akimov *et al.*, in *Nonequilibrium Carrier Dynamics in Semiconductors*, Vol. 110, Proceedings in Physics, edited by M. Saraniti and U. Ravaioli (Springer, Berlin, 2006), pp. 229–232.

[36] E. Alfinito, C. Pennetta, and L. Reggiani, Nanotechnology **19**, 065202 (2008).

[37] E. Alfinito, C. Pennetta, and L. Reggiani, J. Appl. Phys. **105**, 084703 (2009).

[38] J. G. Simmons, J. Appl. Phys. **34**, 1793 (1963).

[39] J. N. Onuchic, Z. Luthey-Schulten, and P. G. Wolynes, Ann. Rev. Phys. Chem. **48**, 545 (1997).

[40] B. K. Kobilka and X. Deupi, Trends Pharmacol. Sci. **28**, 397 (2007).

[41] S. Goutelle, M. Maurin, F. Rougier, X. Barbaut, L. Bourguignon, M. Ducher, and P. Maire, Fundam. Clin. Pharmacol. **22**, 633 (2008).